


Cite this: *RSC Adv.*, 2020, 10, 29263


Received 1st June 2020

Accepted 31st July 2020

DOI: 10.1039/d0ra04816j

rsc.li/rsc-advances

# Rh-catalyzed highly regioselective hydroformylation to linear aldehydes by employing porous organic polymer as a ligand†

Zhaozhan Wang<sup>a</sup> and Yong Yang \*<sup>ab</sup>

In this work, we developed a new structural porous organic polymer containing biphosphoramidite unit, which can be used as a solid bidentate phosphorous ligand for rhodium-catalyzed solvent-free higher olefins hydroformylation. The resultant catalyst demonstrated unprecedentedly high regioselectivity to linear aldehydes and could be readily recovered for successive reuses with good stability in both catalytic activity and regioselectivity.

## Introduction

Hydroformylation, also known as the oxo process, is a highly atom-economical synthetic method to prepare aldehydes by the addition of syngas ( $H_2/CO$ ) into olefins.<sup>1</sup> To date, homogeneous ligand-modified rhodium or cobalt complexes have been successfully used in industry, and more than 10 million tons of aldehydes are produced annually.<sup>2</sup> In particular, rhodium compounds generally give rise to high reaction rates and good selectivity to the desired products. However, industrial applications of these homogeneous catalysts remain a challenge because they are expensive, cannot be recycled, and are difficult to separate from the product mixture. In contrast, the heterogeneous catalysts hold significant advantages, such as easy of catalyst separation and recyclability, compared with homogeneous analogues. More importantly, heterogeneous catalysts can often present different or even unexpected catalytic performance, due to the surface support properties, metal-support interactions, and microenvironments of catalytically active sites.<sup>3</sup>

Due to the commercial interest, the linear aldehydes, as versatile intermediates for the production of plasticizer alcohols, detergents, surfactants and other useful fine chemicals, have been the most desired products for hydroformylation of higher olefins ( $>C_5$ ).<sup>4</sup> To this end, considerable efforts have been devoted in designing new types of phosphorous ligands for rhodium-catalyzed hydroformylation processes. A family of ligands, *e.g.*, xantphos,<sup>5</sup> bisbi,<sup>6</sup> naphos,<sup>7</sup> biphephos,<sup>8</sup> calix[4] arene bisphosphate,<sup>9</sup> spiroketal-based bisphosphoramidite ligands,<sup>10</sup> pyrrole-based tri- and tetra-phosphoramidite

ligands,<sup>11</sup> have been developed and demonstrated high regioselectivities to linear aldehydes. Among them, pyrrole-based phosphoramidites developed firstly by van Leeuwen,<sup>10a</sup> followed by Ding,<sup>10b,c</sup> Zhang,<sup>11a,b</sup> and Chen<sup>11c</sup> respectively, gave unprecedentedly high regioselectivity due to the strong  $\pi$ -acceptor ability of phosphorous. Nonetheless, all cases are still limited to homogeneous catalytic system. Therefore, the development of a heterogeneous catalyst with excellent regioselectivity to linear aldehydes is highly desirable.

Over the past few years, porous organic polymers (POPs) have attracted considerable attention due to their high specific surface areas, porous channels, and adjustable functionalities in their structures.<sup>12</sup> Specifically, some P or N-containing molecule units, serving as coordination sites to ligate with metal species to form catalytically active sites, can be effectively incorporated into the POPs structures. As such, POPs can be employed as solid supports and porous organic ligands (POLs) in catalysis. In this context, Xiao, Ding and co-workers developed POLs bearing a  $PPh_3$  unit to coordinate Rh species to form a heterogeneous supported Rh catalyst (denoted as Rh/POL- $PPh_3$ ), which exhibited superior activity and excellent recyclability for 1-octene hydroformylation.<sup>13</sup> Later on, two groups have independently developed several different POPs-based metal catalysts containing various coordination molecule units for organic transformations.<sup>14</sup> Very recently, POPs-based heterogeneous catalysts have also been expanded for hydrosilylation,<sup>15</sup>  $CO_2$  fixation,<sup>16</sup> and others.<sup>17</sup>

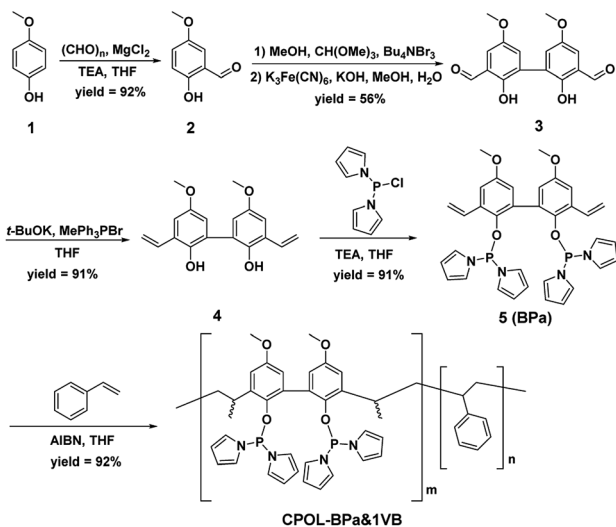
Herein, we report a new porous organic polymers (named as CPOL-BPa&1VB) with biphosphoramidite molecule unit (Scheme 1), which has large surface area with hierarchical pores and can coordinate with Rh species to form a heterogeneous catalyst. The resultant catalyst shows superior activity and excellent regioselectivity to linear aldehydes in hydroformylation of higher olefins. In addition, the catalyst can be readily recovered for successive reuse without appreciable loss of catalytic performance.

<sup>a</sup>CAS Key Laboratory of Bio-Based Materials, Qingdao Institute of Bioenergy and Bioprocess Technology, Chinese Academy of Sciences, Qingdao 266101, China. E-mail: yangyong@qibebt.ac.cn

<sup>b</sup>Dalian National Laboratory for Clean Energy, Dalian 116023, China

† Electronic supplementary information (ESI) available. See DOI: 10.1039/d0ra04816j





Scheme 1 Synthesis of CPOL-BPa&amp;1VB.

## Results and discussion

The **CPOL-BPa&1VB** was prepared *via* copolymerization of divinyl-functionalized pyrrole-based biphosphoramidite (**5**, BPa) with styrene as the monomers under solvothermal conditions, as shown in Scheme 1 (see details in the ESI†). Divinyl diphenol **4** was synthesized from 4-methoxyphenol **1** as starting material followed by sequential formylation, coupling, and Wittig reactions. Divinyl-functionalized pyrrole-based biphosphoramidite **5** was prepared by treatment of **4** with chlorodipyrrolyphosphine in the presence of Et<sub>3</sub>N as a HCl scavenger. **CPOL-BPa&1VB** was obtained in 92% yield by copolymerization of **5** with styrene (St) under solvothermal conditions in tetrahydrofuran (THF) at 100 °C for 48 h in the presence of azobisisobutyronitrile (AIBN). For comparison, copolymerization of **5** with other different structure monomers, such as divinylbenzene (2VB), tris(phenylene)vinylene (3VTPB), and tri(4-vinphenyl)phosphane (3VPPPh<sub>3</sub>), tris(4-vinylphenyl) phosphite (3VTPPi), were also prepared under similar conditions, denoted as **CPOL-BPa&2VB**, **CPOL-BPa&3VTPB**, and **CPOL-BPa&3VPPPh<sub>3</sub>**, **CPOL-BPa&3VTPPi**, respectively.

Comprehensive characterizations were carried out to investigate the local chemical structure of the obtained **CPOL-BPa&1VB**.  $^{13}\text{C}$  MAS NMR spectrum (Fig. 1A) demonstrates that an additional peak at around 42 ppm with strong intensity appears, assignable to the polymerized vinyl groups, accompanying with the appearance of the characteristic peaks attributed to the pyrrole-based biphosphoramidite upon copolymerization. This result strongly suggests the success of copolymerization of **5** and styrene monomer. A single peak at 105.4 ppm without appearance of oxidized phosphorous species was observed in  $^{31}\text{P}$  MAS NMR spectrum (Fig. 1B), which is in well consistent with that of the monomer **5** (see the ESI†), indicating that P species are stable during the copolymerization.  $\text{N}_2$  sorption isotherm (Fig. 1C) shows a sharp uptake of  $\text{N}_2$  at low relative pressure ( $P/P_0 < 0.1$ ) and a hysteresis loop at higher relative

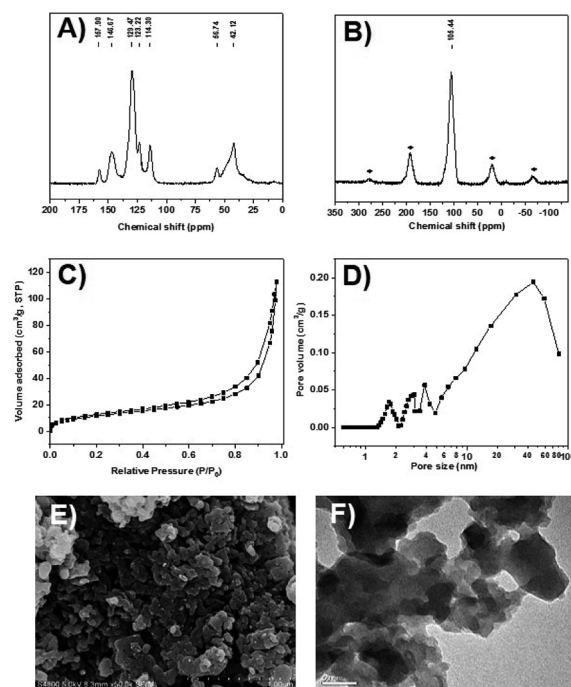


Fig. 1 (A)  $^{13}\text{C}$  MAS NMR spectrum, (B)  $^{31}\text{P}$  MAS NMR spectrum, (C)  $\text{N}_2$  sorption isotherm, (D) pore size distribution calculated by nonlocal density functional theory (NLDFIT), (E) SEM and (F) TEM image of CPOL-BPa6-1VB.

pressure ( $0.4 < P/P_0 < 1.0$ ), indicating the existence of hierarchical micro-, meso-, and macropores in the framework, which was further confirmed by analysis of pore-size distribution (Fig. 1D). The total pore volume and BET surface area derived from  $N_2$  adsorption data were as high as  $0.4 \text{ cm}^3 \text{ g}^{-1}$  and  $140 \text{ m}^2 \text{ g}^{-1}$ , respectively, which should be beneficial for its application as a support to immobilize metal species and in turn facilitate the reaction effectively. Scanning electron microscopy (SEM) and transmission electron microscopy (TEM) images (Fig. 1E and F) display a quite rough surface morphology with presence of hierarchically porous structures in the framework. The thermogravimetric analysis (TGA) (Fig. S1†) shows that the **CPOL-BPa&1VB** has good thermal stability. Upon reaction of  $\text{Rh}(\text{acac})(\text{CO})_2$  with **CPOL-BPa&1VB**, a new peak at 129.8 ppm was observed in the solid state  $^{31}\text{P}$  MAS NMR spectrum (Fig. S2†), assignable to the P species coordinated with Rh with a possible structure of  $\text{HRh}(\text{BPa})_2(\text{CO})$ ,<sup>10a</sup> indicating the success of the coordination.

Subsequently, we treated the **CPOL-BPa1VB** with Rh(acac)(CO)<sub>2</sub> (acac = acetylacetonate) to afford its corresponding Rh catalyst for solvent-free 1-hexene hydroformylation as a benchmark reaction to investigate its catalytic performance, the results are compiled in Table 1. Firstly, a set of parameters, including reaction temperature, reaction time, pressure of syngas, and substrate/catalyst (S/C) ratios were screened intensively. Higher temperature gave an increased reaction efficiency, while lower reaction temperatures dramatically improved the regioselectivity to linear aldehyde together with a reduced product selectivity to hydrogenation and isomerization of 1-

Table 1 Hydroformylation of olefins catalysed by CPOL-BPa&1VB-based Rh catalyst<sup>a</sup>

<div><div><div><div><div><div></div><div><math>\text{R}-\text{CH}=\text{CH}_2</math></div></div></div><div><div><math>\xrightarrow[\text{Rh cat.}]{\text{H}_2 + \text{CO}}</math></div></div><div><div><div><div><div><math>\text{R}-\text{CH}_2\text{CHO}</math></div><div><i>linear</i></div></div><div><div><math>\text{R}-\text{CH}(\text{CH}_3)\text{CHO}</math></div><div><i>branched</i></div></div><div><div><math>\text{R}-\text{CH}=\text{CH}-\text{CH}=\text{CH}_2</math></div><div><i>isomerization</i></div></div><div><div><math>\text{R}-\text{CH}_2\text{CH}_2\text{CH}_3</math></div><div><i>alkane</i></div></div></div></div></div></div></div></div>										
Entry	Olefin	S/C	Temperature (°C)	Time (h)	$P_{\text{H}_2+\text{CO}}$ (MPa)	Conversion <sup>b</sup> (%)	$l/b^b$	Selectivity <sup>b</sup> (%)		
								Aldehyde	Isomerization	Alkane
1	1-Hexene	12 750	60	8	2	79.5	175.7	90.6	5.7	3.6
2	1-Hexene	12 750	80	8	2	98.5	158.5	87.8	6.8	5.4
3	1-Hexene	12 750	100	8	2	99.3	35.7	69.7	6.2	23.9
4	1-Hexene	12 750	80	5	2	91.5	134.9	82.9	10.1	6.9
5	1-Hexene	12 750	80	8	1	96.5	95.7	65.8	16.0	18.2
6	1-Hexene	12 750	80	8	4	94.1	89.0	90.0	6.3	3.7
7	1-Hexene	10 000	80	8	2	99.2	164.0	88.4	7.3	4.3
8	1-Hexene	20 000	80	8	2	91.7	157.0	83.9	9.0	7.1
9	1-Hexene	30 000	80	8	2	70.1	123.0	59.6	22.8	17.6
10	1-Hexene	30 000	80	12	2	96.4	155.3	82.8	9.6	7.6
1 <sup>c</sup>	1-Octene	6710	80	8	2	99.6	104.3	73.7	24.7	1.5
12 <sup>d</sup>	2-Octene	10 107	100	8	2	66.0	8.9	66.8	32.6	0.4
13 <sup>e</sup>	Styrene	13 740	80	15	2	85.0	0.1	95.8	—	4.2

<sup>a</sup> Reaction conditions: 1-hexene (3 mL), CPOL-BPa&1VB (8 mg), Rh(acac)(CO)<sub>2</sub> (0.49 mg), H<sub>2</sub>/CO = 1/1. <sup>b</sup> Determined by GC and GC-MS using decane as an internal standard sample and confirmed with their corresponding authentic samples. <sup>c</sup> 1-Octene (2 mL), toluene (2 mL). <sup>d</sup> 2-Octene (3 mL). <sup>e</sup> Styrene (3 mL).

hexene (entries 1–3). To our surprise, unprecedented regioselectivity to linear 1-heptanal with  $l/b$  ratio up to 158.5 and almost complete conversion of 1-hexene was achieved when the reaction was performed at 80 °C and 2.0 MPa pressure of syngas after 8 h (entry 2). To the best of our knowledge, this is the highest value among all obtained results catalyzed by a heterogeneous Rh catalyst so far. A decrease or increase of pressure of syngas led to relatively lower regioselectivity to linear 1-heptanal with comparable reaction efficiency, while a considerable poorer selectivity to aldehyde was afforded at lower pressure under otherwise identical conditions (entries 5 and 6). Survey of different substrate/catalyst (SC) ratios ranging from 10 000 to 30 000 for the reaction reveals no appreciable changes in regioselectivity to linear 1-heptanal, while a slight longer reaction time was required to guarantee complete conversion, higher selectivity, and excellent regioselectivity to 1-heptanal for the reaction with higher S/C ratio (entries 2, 7–10).

Under the optimized conditions, we next investigated other olefins hydroformylation. Longer chain 1-octene could be efficiently hydroformylated, affording excellent regioselectivity to linear aldehyde with  $l/b$  ratio of 104.3 in full conversion (entry 11). Internal 2-octene was also suitable for this reaction conditions, while a considerably lower  $l/b$  ratio (8.9) of aldehyde was achieved in this case (entry 12). Besides, styrene, as a functionalized olefin, was also compatible, giving the branched aldehyde as major product ( $l/b = 0.10$ ) in excellent selectivity with TON as high as 11 680 (entry 13).

For comparison, 5 was used as a ligand for the homogeneous hydroformylation under otherwise identical conditions. It turns out that nearly equal reaction efficiency to that of Rh/CPOL-BPa&1VB was achieved, but with a considerably lower regioselectivity to linear 1-heptanal ( $l/b = 33.0$  vs. 158.5) (Table 2, entry

1). Such a result not only clearly indicates that CPOL-BPa&1VB can achieve equal level of reaction efficiency as a homogeneous counterpart, but also showcases that the created

Table 2 Comparative results for 1-hexene hydroformylation using different ligands<sup>a</sup>

$\text{CH}_3(\text{CH}_2)_4\text{CH=CH}_2 \xrightarrow[\text{Rh cat.}]{\text{H}_2 + \text{CO}} \text{CH}_3(\text{CH}_2)_4\text{CH}_2\text{CHO} + \text{CH}_3(\text{CH}_2)_3\text{CH}(\text{CH}_3)\text{CHO} + \text{CH}_3(\text{CH}_2)_3\text{CH=CH}_2 + \text{CH}_3(\text{CH}_2)_5\text{CH}_3$ <div style="display: flex; justify-content: space-around; font-size: small;"> <span>1</span> <span>2</span> <span>3</span> <span>4</span> </div>									
Entry	Ligand	Conversion <sup>b</sup> (%)	$l/b^b$	Selectivity <sup>b</sup> (%)				1 + 2	3 + 4
				1	2	3	4		
1	5 (BPa)	99.4	33.0	85.1	2.5	12.4			
2 <sup>c</sup>	—	98.5	1.2	25.7	13.7	60.6			
3	CPOL-BPa&1VB	98.5	158.5	87.8	6.8	5.4			
4	CPOL-BPa&2VB	99.4	82.9	55.7	13.4	30.9			
5	CPOL-BPa&3VTPB	89.5	31.1	86.6	6.8	6.6			
6	CPOL-BPa&3VPPH <sub>3</sub>	86.3	13.7	88.2	6.0	5.8			
7	CPOL-BPa&3VTPPi	97.5	10.1	90.7	4.1	5.2			

<sup>a</sup> Reaction conditions: 1-hexene (3 mL), Rh(acac)(CO)<sub>2</sub> (0.49 mg), H<sub>2</sub>/CO pressure (2 MPa, H<sub>2</sub>/CO = 1/1), 80 °C, CPOL-BPa&1VB (8 mg), CPOL-BPa&2VB (18.2 mg), CPOL-BPa&3VTPB (42.4 mg), CPOL-BPa&3VPPH<sub>3</sub> (19.1 mg), CPOL-BPa&3VTPPi (21.4 mg). <sup>b</sup> Determined by GC and GC-MS using decane as an internal standard sample and confirmed with their corresponding authentic samples. <sup>c</sup> In the absence of ligand.



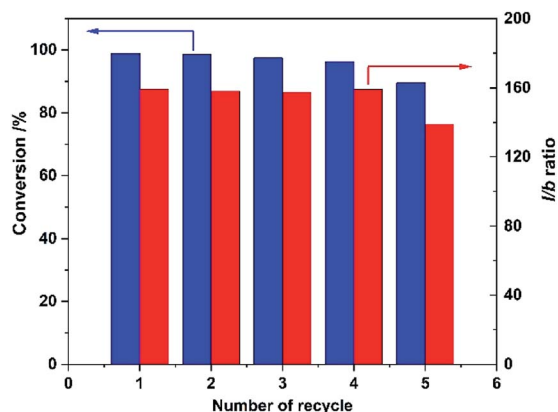


Fig. 2 Recyclability of Rh/CPOL-BPa&1VB for 1-hexene hydroformylation under the optimized conditions.

microenvironment of catalytically active sites can unexpectedly tune the catalytic performance. However, in the absence of ligand, 1-hexene was converted into hexane as major product with poor selectivity to 1-heptanal (Table 2, entry 2).

Furthermore, several different structural CPOLs (e.g., CPOL-BPa&2VB, CPOL-BPa&3VTPB, CPOL-BPa&3VPPH<sub>3</sub>, CPOL-BPa&3VTPPi) were employed as solid ligands derived from copolymerization of 5 with varying vinyl-functionalized molecules as monomers (Table 2). The combination of Rh(acac)(CO)<sub>2</sub> with these solid ligands demonstrated nearly comparable catalytic reactivity but with huge differences in regioselectivity to linear 1-heptanal under the optimized conditions. Among all investigated CPOLs, the CPOL-BPa&1VB stood out, affording the highest regioselectivity to linear 1-heptanal.

Finally, recyclability of the Rh/CPOL-BPa&1VB was investigated using the hydroformylation of 1-hexene under the optimized conditions. After each reaction, the solid catalyst was separated by centrifugation, washed with methanol and dried for next reaction. As shown in Fig. 2, both the catalytic activity and regioselectivity to linear 1-heptanal was remained without significant change after 5 recycles, indicating its high stability of the catalyst.

## Conclusions

In conclusion, we developed a new porous organic polymer (POP) with large surface area and hierarchical pores via copolymerization of bivinyl-functionalized pyrrole-based biphosphoramidite with styrene under solvothermal conditions. The polymer contains biphosphoramidite molecule unit and can be used as a solid support and ligand for Rh-catalyzed solvent-free higher olefins hydroformylation, which demonstrates outstanding activity and unprecedentedly high regioselectivity to linear aldehydes. More importantly, the resultant catalyst can be readily recovered for successive reuse with good maintenance of both catalytic activity and regioselectivity.

## Conflicts of interest

There are no conflicts to declare.

## Acknowledgements

This work was supported DICP & QIBEBT (Grant No. DICP & QIBEBT UN201704, QIBEBT I201902), and the Dalian National Laboratory for Clean Energy (DNL) Cooperation Fund, Chinese Academy of Sciences (Grant No. DNL201904).

## Notes and references

- 1 B. Breit, *Top. Curr. Chem.*, 2007, **279**, 139–172.
- 2 R. Franke, D. Selent and A. Börner, *Chem. Rev.*, 2012, **112**, 5675–5732.
- 3 (a) J. Zhang, P. Sun, Z. Zhao, G. Gao and F. Li, *Chin. Sci. Bull.*, 2019, **64**, 1–15; (b) P. Dydio, W. I. Dzik, M. Lutz, B. de Bruin and J. N. H. Reek, *Angew. Chem., Int. Ed.*, 2011, **50**, 396–400.
- 4 E. V. Gusevskaya, J. Jiménez-Pinto and A. Börner, *ChemCatChem*, 2014, **6**, 382–411.
- 5 M. Kranenburg, Y. E. M. van der Burgt, P. C. J. Kamer and P. W. N. M. van Leeuwen, *Organometallics*, 1995, **14**, 3081–3089.
- 6 T. J. Devon, G. W. Phillips, T. A. Puckette, J. L. Stavinoha and J. J. Vanderbilt, *US Pat.*, 4694109, 1987.
- 7 H. Klein, R. Jackstell, K. D. Wiese, C. Borgmann and M. Beller, *Angew. Chem., Int. Ed.*, 2001, **40**, 3408–3411.
- 8 E. Billig, A. G. Abatjoglou and D. R. Bryant, *US Pat.*, 4668651 (1987) and 4769498 (1988).
- 9 R. Paciello, L. Siggel and M. Röper, *Angew. Chem., Int. Ed.*, 1999, **38**, 1920–1923.
- 10 (a) S. C. van der Slot, J. Duran, J. Luten, P. C. J. Kamer and P. W. N. M. van Leeuwen, *Organometallics*, 2002, **21**, 3873–3883; (b) X. Jia, Z. Wang, C. Xia and K. Ding, *Chem.-Eur. J.*, 2012, **18**, 15288–15295; (c) X. Ren, Y. Zheng, L. Zhang, Z. Wang, C. Xia and K. Ding, *Angew. Chem., Int. Ed.*, 2017, **56**, 310–313.
- 11 (a) S. Yu, Y. Chie, Z. Guan and X. Zhang, *Org. Lett.*, 2008, **10**, 3469–3472; (b) C. Chen, Y. Qiao, H. Geng and X. Zhang, *Org. Lett.*, 2013, **15**, 1048–1051; (c) W. Han, S. Qin, X. Shu, Q. Wu, B. Xu, R. Li, X. Zheng and H. Chen, *RSC Adv.*, 2016, **6**, 53012–53016.
- 12 (a) L. Chen, Y. Yang and D. Jiang, *J. Am. Chem. Soc.*, 2010, **132**, 9138–9143; (b) P. Kaur, J. T. Hupp and S. T. Nguyen, *ACS Catal.*, 2011, **1**, 819–835; (c) Y. Zhang and J. Y. Ying, *ACS Catal.*, 2015, **5**, 2681–2691; (d) Q. Sun, Z. Dai, X. Meng, L. Wang and F. Xiao, *ACS Catal.*, 2015, **5**, 4556–4567; (e) A. G. Slater and A. I. Cooper, *Science*, 2015, **348**, aaa8075; (f) G. Liu, Y. Wang, C. Shen, Z. Ju and D. Yuan, *J. Mater. Chem. A*, 2015, **3**, 3051–3058; (g) Q. Sun, Z. Dai, X. Meng and F.-S. Xiao, *Chem. Soc. Rev.*, 2015, **44**, 6018–6034.
- 13 Q. Sun, M. Jiang, Z. Shen, Y. Jin, S. Pan, L. Wang, X. Meng, W. Chen, Y. Ding, J. Li and F.-S. Xiao, *Chem. Commun.*, 2014, **50**, 11844–11847.
- 14 (a) Q. Sun, Z. Dai, X. Liu, N. Sheng, F. Deng, X. Meng and F.-S. Xiao, *J. Am. Chem. Soc.*, 2015, **137**, 5204–5209; (b) Q. Sun, B. Aguila, G. Verma, X. Liu, Z. Dai, F. Deng, X. Meng, F.-S. Xiao and S. Ma, *Chem*, 2016, **1**, 628–639; (c) C. Li, K. Xiong, L. Yan, M. Jiang, X. Song, T. Wang, X. Chen, Z. Zhan and Y. Ding, *Catal. Sci. Technol.*, 2016, **6**,



- 2143–2149; (d) C. Li, L. Yan, L. Lu, K. Xiong, W. Wang, M. Jiang, J. Liu, X. Song, Z. Zhan, Z. Jiang and Y. Ding, *Green Chem.*, 2016, **18**, 2995–3005; (e) Y. Wang, L. Yan, C. Li, M. Jiang, Z. Zhao, G. Hou and Y. Ding, *J. Catal.*, 2018, **368**, 197–206; (f) C. Li, K. Sun, W. Wang, L. Yan, X. Sun, Y. Wang, K. Xiong, Z. Zhan, Z. Jiang and Y. Ding, *J. Catal.*, 2017, **353**, 123–132; (g) Z. Ren, Y. Lium, Y. Lyu, X. Song, C. Zheng, S. Feng, Z. Jiang and Y. Ding, *J. Catal.*, 2019, **369**, 249–256.
- 15 (a) R.-H. Li, X.-M. An, Y. Yang, D.-C. Li, Z.-L. Hu and Z.-P. Zhan, *Org. Lett.*, 2018, **20**, 5023–5026; (b) R.-H. Li, G.-L. Zhang, J.-X. Dong, D.-C. Li, Y. Yang, Y.-M. Pan, H.-T. Tang, L. Chen and Z.-P. Zhang, *Chem.-Asian J.*, 2019, **14**, 149–154.
- 16 W. Wang, Y. Wang, C. Li, L. Yan, M. Jiang and Y. Ding, *ACS Sustainable Chem. Eng.*, 2017, **5**, 4523–4528.
- 17 (a) R. Jana and J. A. Tunge, *J. Org. Chem.*, 2011, **76**, 8376–8385; (b) Y.-B. Zhou, Y.-Q. Wang, L. C. Ning, Z.-C. Ding, W.-L. Wang, C.-K. Ding, R.-H. Li, J.-J. Chen, X. Lu, Y.-J. Ding and Z.-P. Zhan, *J. Am. Chem. Soc.*, 2017, **139**, 3966–3969; (c) R. Cai, X. Ye, Q. Sun, Q. He, Y. He, S. Ma and X. Shi, *ACS Catal.*, 2017, **7**, 1087–1092.

